

See discussions, stats, and author profiles for this publication at: <https://www.researchgate.net/publication/51495165>

Capture of Nerve Agents and Mustard Gas Analogues by Hydrophobic Robust MOF-5 Type Metal–Organic Frameworks

ARTICLE *in* JOURNAL OF THE AMERICAN CHEMICAL SOCIETY · AUGUST 2011

Impact Factor: 12.11 · DOI: 10.1021/ja2042113 · Source: PubMed

CITATIONS

74

READS

65

9 AUTHORS, INCLUDING:



Carmen Montoro

Universidad Autónoma de Madrid

15 PUBLICATIONS 342 CITATIONS

SEE PROFILE



Elsa Quartapelle

University of Milan

18 PUBLICATIONS 373 CITATIONS

SEE PROFILE



Irena Senkovska

Technische Universität Dresden

90 PUBLICATIONS 2,824 CITATIONS

SEE PROFILE



Stefan Kaskel

Technische Universität Dresden

293 PUBLICATIONS 6,586 CITATIONS

SEE PROFILE

Capture of Nerve Agents and Mustard Gas Analogues by Hydrophobic Robust MOF-5 Type Metal–Organic Frameworks

Carmen Montoro,[†] Fátima Linares,[†] Elsa Quartapelle Procopio,[†] Irena Senkovska,[‡] Stefan Kaskel,[‡] Simona Galli,[§] Norberto Masciocchi,[§] Elisa Barea,^{*,†} and Jorge A. R. Navarro^{*,†}[†]Departamento de Química Inorgánica, Universidad de Granada, Av. Fuentenueva S/N, 18071 Granada, Spain[‡]Department of Inorganic Chemistry, Dresden University of Technology, Mommsenstrasse 6, 01069 Dresden, Germany[§]Dipartimento di Scienze Chimiche e Ambientali, Università dell'Insubria, Via Valleggio 11, 22100 Como, Italy

S Supporting Information

ABSTRACT: In this communication, a series of observations and data analyses coherently confirms the suitability of the novel metal–organic framework (MOF) $[\text{Zn}_4(\mu_4\text{-O})(\mu_4\text{-4-carboxy-3,5-dimethyl-4-carboxy-pyrazolato})_3]$ (**1**) in the capture of harmful volatile organic compounds (VOCs). It is worthy of attention that **1**, whose crystal structure resembles that of MOF-5, exhibits remarkable thermal, mechanical, and chemical stability, as required if practical applications are sought. In addition, it selectively captures harmful VOCs (including models of Sarin and mustard gas, which are chemical warfare agents), even in competition with ambient moisture (i.e., under conditions mimicking operative ones). The results can be rationalized on the basis of Henry constant and adsorption heat values for the different essayed adsorbates as well as $\text{H}_2\text{O}/\text{VOC}$ partition coefficients as obtained from variable-temperature reverse gas chromatography experiments. To further strengthen the importance of **1**, its performance in the capture of harmful VOCs has been compared with those of well-known materials, namely, a MOF with coordinatively unsaturated metal sites, $[\text{Cu}_3(\text{btc})_2]$ and the molecular sieve active carbon Carboxen. The results of this comparison show that coordinatively unsaturated metal sites (preferential guest-binding sites) are ineffective for the capture of VOCs in the presence of ambient moisture. Consequently, we propose that the driving force of the VOC–MOF recognition process is mainly dictated by pore size and surface hydrophobicity.

Protection against fortuitous or deliberate emissions of harmful chemical compounds is of major social concern. Particularly, protection against readily accessible chemical warfare agents such as Sarin nerve gas and mustard vesicant gas is definitely necessary. In this regard, the availability of high-performance materials for sensing, capturing, or decomposing^{1,2} chemical warfare agents is of undoubted interest.

The selective adsorptive³ and catalytic⁴ properties of porous metal–organic frameworks (MOFs) are very attractive for the capture and/or decomposition of harmful volatile organic compounds (VOCs).^{5,6} Nevertheless, to the best of our knowledge, only one report on the possible utility of MOFs for chemical warfare protection, dealing with the solid–liquid adsorption process of an anionic organophosphate nerve agent surrogate, has appeared in the scientific literature.⁷

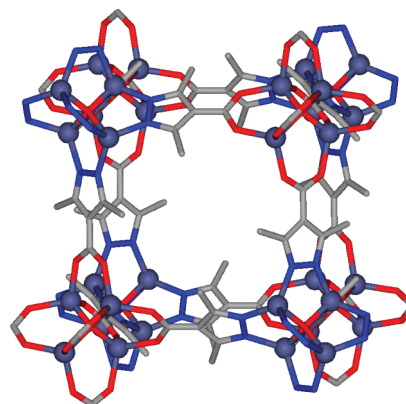
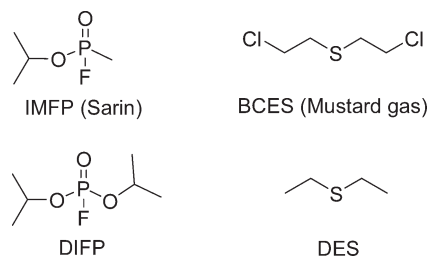


Figure 1. Idealized view of a portion of the crystal structure of $[\text{Zn}_4\text{O}(3,5\text{-dimethyl-4-carboxypyrazolato})_3]$ (**1**) with segregated $\text{Zn}_4\text{O}(\text{CO}_2)_6$ and $\text{Zn}_4\text{O}(\text{pz})_3$ SBUs.

Scheme 1. Chemical Warfare Agents Isopropylmethylfluorophosphate (IMFP, Sarin Nerve Gas), and Bis(2-chloroethyl)sulfide (BCES, Mustard Vesicant Gas) and the Corresponding Model Compounds Used in Our Studies (DIFP, Diisopropylfluorophosphate; DES, diethylsulfide)



In this communication, we report a proof of concept of the use of hydrophobic MOFs to capture chemical warfare agents. Indeed, the novel robust MOF $[\text{Zn}_4\text{O}(3,5\text{-dimethyl-4-carboxypyrazolato})_3]$ (**1**) (Figure 1) is able to capture model compounds of Sarin nerve gas and Mustard vesicant gas (Scheme 1) from the gas phase.

Received: May 7, 2011

Published: July 14, 2011

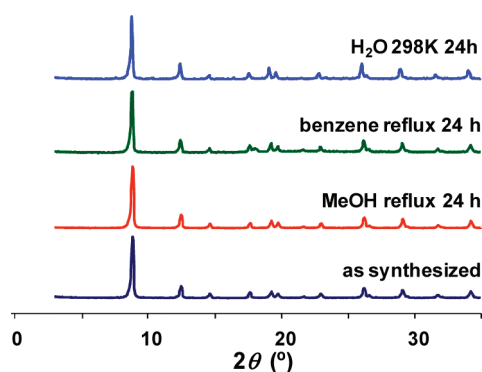


Figure 2. Chemical stability tests on **1** suspended in water at room temperature and in boiling organic solvents for 24 h.

1 can easily be prepared in large amounts and high yields (up to 20 g per batch) as a microcrystalline material by the direct reaction of $\text{Zn}(\text{NO}_3)_2$ with 3,5-dimethyl-4-carboxypyrazole (H_2dmcapz) in a basic ethanol medium under reflux. **1** crystallizes in the cubic $Fm\text{-}3m$ space group.⁸ Within its three-dimensional porous framework, Zn_4O^{6+} tetranuclear nodes are connected to six symmetry-related ones by (50% orientationally disordered) N,N',O,O' -*exo*-tetradentate 3,5-dimethyl-4-carboxypyrazolato spacers. Rather narrow windows (less than $4 \text{ \AA} \times 4 \text{ \AA}$) give access to pores with diameters of $\sim 6 \text{ \AA}$ ⁹ comprising, after solvent removal, a void volume of $\sim 47\%$. The protrusion of the methyl groups into the pores is reasonably responsible for the high hydrophobicity featured by **1** (see below) and possibly contributes to its chemical inertness by protecting the $\text{M}-\text{O}$ (carboxylate) bonds from hydrolysis. When the symmetry is reduced to the $F23$ space group (i.e., when the disorder is eliminated), the framework possesses a rock salt-type topology in which $\text{M}_4\text{O}(\text{CO}_2)_6$ and $\text{M}_4\text{O}(\text{pz})_3$ secondary building units (SBUs) are joined by the dmcapz spacers (Figure 1). Accordingly, the structure of **1** is reminiscent of that of the renown $[\text{Zn}_4\text{O}(\text{1,4-benzenedicarboxylato})_3]$ system (MOF-5),¹⁰ the disorder observed in **1** being retraceable to the nearly equal coordination features of the N - and O -ends of the dmcapz ligand.

The utility of MOF-5 for practical applications is hampered by the easy hydrolysis of the $\text{Zn}-\text{O}$ coordinative bonds, which makes the whole framework extremely sensitive to moisture.¹¹ This drawback can be limited by substituting the carboxylate ligands with structurally related N -donor spacers (tetrazolates, triazolates, pyrazolates), which afford materials with enhanced thermal and chemical stability as a consequence of the greater robustness of the $\text{M}-\text{N}$ bonds.^{6,12,13} In the case of **1**, which contains a hybrid N,O -donor ligand, we assessed its robustness by performing a series of thermal assays as well as chemical and mechanical stability tests. Significantly, **1** resisted key treatments such as suspension in distilled water or a slightly acidic medium (0.001 M HNO_3) at room temperature or in a boiling organic solvent (methanol, benzene, or cyclohexane) for a prolonged period of time (Figure 2). Only after severe heating in water at 80°C for 8 h was the formation of a (still uncharacterized) dense material formulated as $[\text{Zn}_3(\text{OH})_2(\text{dmcapz})_2]$ (**2**) observed. On the other hand, the thermal analyses performed on **1** [thermogravimetric analysis, differential scanning calorimetry, and thermogravimetric measurements (TXRPD)] in a reactive atmosphere of air indicated its outstanding thermal robustness, with decomposition beginning only at 773 K . TXRPD experiments

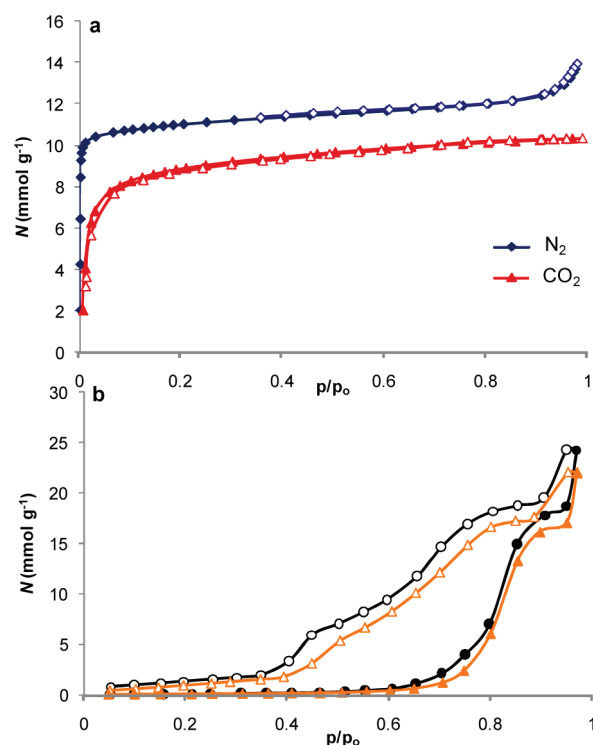


Figure 3. (a) N_2 (77 K, blue diamonds) and CO_2 (195 K, red triangles) adsorption isotherms for **1**; (b) H_2O physisorption isotherm at 298 K (first cycle, black circles; second cycle, brown triangles) for **1**. Solid and open symbols denote adsorption and desorption, respectively.

not only highlighted that **1** preserves its structural features and high crystallinity up to pyrolysis but also were indicative of the framework rigidity: the unit cell volume underwent a very small decrease of -0.5% upon heating [see the Supporting Information (SI)]. The mechanical stability of **1** is also remarkably high, as this material remained practically unaffected after the application of pressures up to 0.2 GPa , which induced a decrease of $\sim 20\%$ in the specific surface area. In contrast, under similar conditions, the highly porous MOFs $[\text{Cr}_3\text{F}(\text{H}_2\text{O})_2\text{O}(\text{1,4-benzenedicarboxylato})_3]$ (MIL-101)¹⁴ and $[\text{Cu}_3(1,3,5\text{-benzenetricarboxylato})_2]$ ($[\text{Cu}_3(\text{btc})_2]$)¹⁵ underwent significant amorphization, with loss of up to 90% of the original porosity (see the SI).

The accessibility of guest molecules into the porous network of **1** was assessed by solid–gas adsorption experiments involving different probe gases, namely, N_2 (77 K), CO_2 (195 K), and H_2O (298 K) (Figure 3). The N_2 and CO_2 adsorption isotherms exhibit type-I behavior, which is typical of crystalline microporous materials, with BET specific surface areas of 840 and $740 \text{ m}^2 \text{ g}^{-1}$, respectively. The adsorption capacity of the micropores is quite high: $\sim 12 \text{ mmol of N}_2 \text{ g}^{-1}$, corresponding to a micropore volume of $0.45 \text{ cm}^3 \text{ per cm}^3$ of **1**. It is noteworthy that H_2O adsorption at 298 K takes place only at very high relative pressures ($p/p_0 > 0.7$), which is indicative of a highly hydrophobic material that is possibly adequate for the adsorption of VOCs. The total pore volume calculated from the water adsorption isotherm amounted to $0.40 \text{ cm}^3 \text{ per cm}^3$ of **1**. The high reproducibility of the H_2O adsorption isotherms in multiple cycles further supports the high stability of **1** toward hydrolysis.

The hydrophobic nature of **1** prompted us to investigate its utility for the capture of harmful VOCs. These studies were

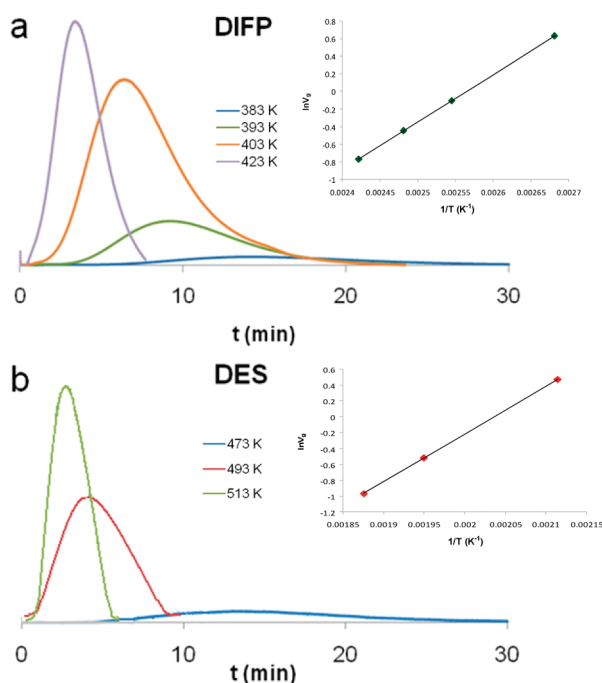


Figure 4. Variable-temperature pulse gas chromatograms for (a) DIFP and (b) DES passed through a chromatographic column packed with **1** using a He flow of 30 mL min^{−1}. The insets represent the variation of the retention volume V_g (in cm³ g^{−1}) as a function of the adsorption temperature (383–513 K).

Table 1. Calculated Heats of Adsorption ΔH_{ads} (kJ mol^{−1}), Henry Constants K_H (cm³ m^{−2}), and Partition Coefficients K_r for **1** with Various VOCs and Water

VOC	$-\Delta H_{\text{ads}}$	K_H^a	K_r^a
DES	50.1	2850	9950
DIFP	44.8	71.2	275
BZ	48.2	1090	4170
CH	9.4	0.07	0.24
H ₂ O	17.9	0.26	—

^a Calculated values at 298 K. Values of K_r for VOCs vs H₂O were obtained from variable-temperature zero-coverage gas chromatography experiments on **1**. Abbreviations: DIFP, diisopropylfluorophosphate; DES, diethylsulfide; BZ, benzene; CH, cyclohexane.

carried out by means of pulse gas chromatography¹⁶ and measurement of breakthrough curves.¹⁷ The variable-temperature pulse gas chromatography studies revealed high retention times for benzene and the chemical warfare agent models DIFP and DES (Figure 4 and Table 1), indicative of a strong interaction of this type of adsorbate with the porous framework of **1**. In contrast, cyclohexane and water vapor were characterized by very low retention times. The weak interaction of cyclohexane with **1** is probably related to its average molecular diameter (>6 Å), which is larger than the small pore windows of **1**, while the weak interaction of H₂O with **1** agrees once again with the hydrophobic nature of this MOF (see above).

To quantify the strength of the interaction of these guest molecules with **1**, we calculated their zero-coverage adsorption heats (ΔH_{ads}) from the variation of the retention volumes (V_g) as a function of temperature according to the equation $\Delta H_{\text{ads}} =$

Table 2. Calculated Heats of Adsorption ΔH_{ads} (kJ mol^{−1}), Henry Constants K_H (cm³ m^{−2}), and partition coefficients K_r for [Cu₃(btc)₂] and Carboxen with Various VOCs and Water

Adsorbent	VOC	$-\Delta H_{\text{ads}}$	K_H^a	K_r^a
[Cu ₃ (btc) ₂]	DES	78.1	6570	116
[Cu ₃ (btc) ₂]	DIFP	48.4	67.9	1.2
[Cu ₃ (btc) ₂]	H ₂ O	43.9	56.3	—
Carboxen	DES	49.0	1170	58000
Carboxen	DIFP	38.3	76.9	3800
Carboxen	H ₂ O	2.7	0.02	—

^a Calculated values at 298 K. Values of K_r for VOCs vs H₂O were obtained from variable-temperature zero-coverage gas chromatography experiments on [Cu₃(btc)₂] and Carboxen.

$-R[\partial(\ln V_g)/\partial(1/T)]$.¹⁸ The direct relation between the retention volume (V_g) and the Henry constant (K_H) also permitted values of the Henry constant under ambient conditions (298 K) to be calculated (Table 1). The high values of ΔH_{ads} and K_H in the case of benzene and the essayed chemical warfare agent models further indicate the strength of their interaction with **1**. On the other hand, the low affinity of this material for water vapor gives rise to very high VOC/H₂O partition coefficients (K_r), suggesting that ambient moisture should not hamper the incorporation of VOCs into **1**. As a matter of fact, breakthrough curve measurements performed on **1** with streams of benzene under both dry and humid conditions supported the effectiveness of this material for VOC capture at room temperature (293 K) even in the presence of moisture (see the SI): The use of a 10 mL min^{−1} He stream containing 130 ppm benzene under dry conditions gave rise to an adsorption of 130 mg of benzene per gram of **1**. When **1** was previously exposed to open air for 48 h, thus mimicking actual operating conditions, flowing a stream of He containing 130 ppm benzene and 50% moisture still induced a significant adsorption of this VOC (60 mg g^{−1}), confirming that ambient moisture is not a strong competitor.

To assess the significance of these results, we studied the performance of cornerstone porous materials toward the capture of the essayed VOCs. To this purpose, we selected a MOF with coordinatively unsaturated metal centers, [Cu₃(btc)₂], and an activated carbon material, Carboxen adsorbent from Sigma-Aldrich. The rationale behind this selection was the following: [Cu₃(btc)₂] is recognized as an outperforming material for the capture of the sulfur-containing VOC tetrahydrothiophene under dry conditions as a consequence of sulfur coordination to the unsaturated Cu centers.⁵ The activated-carbon Carboxen adsorbent possesses pore sizes of 4–8 Å, which are adequate for the selective capture of the studied VOCs, and a specific surface area (485 m² g^{−1}) similar to that of **1**. The variable-temperature zero-coverage adsorption measurements on [Cu₃(btc)₂] and Carboxen are summarized in Table 2. The zero-coverage adsorption heats and values of the Henry constant for Carboxen are very similar to those obtained for **1**, thus suggesting similar adsorption processes dominated by the small size and apolar nature of the pores in the two materials. At variance, the ΔH_{ads} and K_H values for [Cu₃(btc)₂] when probed using DES, DIFP, and H₂O are remarkably higher than those obtained for **1** and Carboxen as a consequence of the interaction of these probe molecules with the coordinatively unsaturated metal centers through their S- and O-donor sites, respectively. It is worthy of note that the high affinity of water toward Cu(II) in [Cu₃(btc)₂] induces very low

VOC/H₂O partition coefficients: this unfortunate effect, manifested by the unequivocal color change from deep-purple to light-blue when [Cu₃(btc)₂] pellets are exposed to ambient moisture, definitely hampers the usefulness of this material under ambient conditions. Accordingly, when hydrated [Cu₃(btc)₂] was placed in the chromatographic column, neither DES nor DIFP were retained under ambient conditions. It should be noted that DES retention by [Cu₃(btc)₂] should be favored by its high DES/H₂O *K_r*; since this was not the case, we can conclude that thermodynamic equilibrium was not reached under the essayed dynamic conditions.⁶ In contrast, as expected on the basis of their hydrophobic nature, both Carboxen and **1** did retain DES under humid conditions.

Of particular interest are the results obtained for the interaction of the porous materials under investigation with DIFP, the analogue of highly toxic Sarin gas. In this regard, it should be noted that human exposure to 50–100 ppb concentration levels of Sarin for 1 min by inhalation or 100–500 mg through the skin are lethal.¹⁹ For an atmosphere containing 50% humidity at 298 K, the water/Sarin ratio should be maintained above the 100–200 range. Hence, only hydrophobic adsorbents like Carboxen or **1** with *K_r*(DIFP/H₂O) > 200 would be effective in maintaining sufficiently low DIFP levels. In contrast, [Cu₃(btc)₂], with *K_r*(DIFP/H₂O) = 1.2, would be not useful for Sarin removal under ambient conditions.

The scalable and environmentally friendly synthesis of **1** and its remarkable chemical, mechanical, and thermal stability granted by the robust nature of the M–N,O(carboxypyrazolato) coordinative bonds are strategic aspects for the application of MOF materials in key technological and industrial fields. In this regard, the prominent affinity and selectivity of the porous structure of **1** for small harmful VOCs might be of paramount importance: as described above, its hydrophobic nature results in large VOC/H₂O partition coefficients, making it definitely appropriate for sustaining actual application conditions in air/gas purification equipment that are well beyond those for the renowned MOF [Cu₃(btc)₂]. Notably, the performance of **1** approaches that of the carbon molecular sieve adsorbent Carboxen. In this regard, it should be noted that the synthesis of **1** is carried out under advantageous mild conditions in comparison with the elaborate preparation of carbon molecular sieves, which require high temperatures and the use of harmful precursors.²⁰ Work can be anticipated in the direction of building membranes and filters containing **1** as well as extending our studies to new MOFs with optimized performance (e.g., higher hydrophobicity, stability, adsorption capacity, and catalytic activity) useful for scavenging of VOCs.

■ ASSOCIATED CONTENT

S Supporting Information. Experimental methods, thermal analyses, chemical stability tests, mechanical stress tests, and gas adsorption breakthrough curves. This material is available free of charge via the Internet at <http://pubs.acs.org>.

■ AUTHOR INFORMATION

Corresponding Author

ebaream@ugr.es; jarn@ugr.es

■ ACKNOWLEDGMENT

Generous support by the Spanish MCINN (Grant CTQ2008-00037/PPQ and Ramon y Cajal Contract to E.B.), the Junta de

Andalucía, and the EU (NanoMOF-228604) is acknowledged. The authors are very grateful for the valuable comments raised by the reviewers.

■ REFERENCES

- (1) Dale, T. J.; Rebek, J., Jr. *Angew. Chem., Int. Ed.* **2009**, *48*, 7850.
- (2) Wagner, G. W.; Bartram, P. W. *J. Mol. Catal. A: Chem.* **1999**, *144*, 419.
- (3) (a) Li, J.-R.; Ma, Y.; McCarthy, M. C.; Sculley, J.; Yu, J.; Jeong, H.-K.; Balbuena, P. B.; Zhou, H.-C. *Coord. Chem. Rev.* **2011**, *255*, 1791. (b) Xiang, S.-C.; Zhang, Z.; Zhao, C.-G.; Hong, K.; Zhao, X.; Ding, D.-R.; Xie, M.-H.; Wu, C.-D.; Das, M. C.; Gill, R.; Thomas, K. M.; Chen, B. *Nat. Commun.* **2011**, *2*, 204.
- (4) For example, see: (a) Feréy, G. *Chem. Soc. Rev.* **2008**, *37*, 191. (b) Farrusseng, D.; Aguado, S.; Pinel, C. *Angew. Chem., Int. Ed.* **2009**, *48*, 7502. (c) Corma, A.; García, H.; Llabrés i Xamena, F. X. *Chem. Rev.* **2010**, *110*, 4606.
- (5) Britt, D.; Tranchemontagne, D. J.; Yaghi, O. M. *Proc. Natl. Acad. Sci. U.S.A.* **2008**, *105*, 11623.
- (6) Galli, S.; Masciocchi, N.; Colombo, V.; Maspero, A.; Palmisano, G.; López-Garzón, F. J.; Domingo-García, M.; Fernández-Morales, I.; Barea, E.; Navarro, J. A. R. *Chem. Mater.* **2010**, *22*, 1664.
- (7) Zou, R.; Zhong, R.; Han, S.; Xu, H.; Burrell, A. K.; Henson, N.; Cape, J. L.; Hickmott, D. D.; Timofeeva, T. V.; Larson, T. E.; Zhao, Y. *J. Am. Chem. Soc.* **2010**, *132*, 17996.
- (8) Relevant crystal data for [Zn₄O(C₆H₆N₂O₂)₃] (**1**): fw = 691.9 g mol⁻¹; cubic, space group *Fm* $\bar{3}$ *m*; *a* = 20.1581(3) Å; *V* = 8191.2(3) Å³; *Z* = 8; *F*(000) = 2752; ρ = 0.98 g cm⁻³; μ (Cu K α) = 27.5 mm⁻¹; *R_p* = 0.073, *wR_p* = 0.101, *R_{Bragg}* = 0.047; CCDC 817665.
- (9) Eufri, D.; Sironi, A. *J. Mol. Graphics* **1989**, *7*, 165.
- (10) Deng, H.; Doonan, C. J.; Furukawa, H.; Ferreira, R. B.; Towne, J.; Knobler, C. B.; Wang, B.; Yaghi, O. M. *Science* **2010**, *327*, 846.
- (11) Proch, S.; Herrmannsdorfer, J.; Kempe, R.; Kern, C.; Jess, A.; Seyfarth, L.; Senker, J. *Chem.—Eur. J.* **2008**, *14*, 8204.
- (12) Tonigold, M.; Lu, Y.; Bredenkötter, B.; Rieger, B.; Bahnmüller, S.; Hitzbleck, J.; Langstein, G.; Volkmer, D. *Angew. Chem., Int. Ed.* **2009**, *48*, 7456.
- (13) Choi, H. J.; Dincă, M.; Dailly, A.; Long, J. R. *Energy Environ. Sci.* **2010**, *3*, 117.
- (14) Feréy, G.; Mellot-Draznieks, C.; Serre, C.; Millange, F.; Dutour, J.; Surble, S.; Margiolaki, I. *Science* **2005**, *309*, 2040.
- (15) Chui, S. S. Y.; Lo, S. M. F.; Charmant, J. P. H.; Orpen, A. G.; Williams, I. D. *Science* **1999**, *283*, 1148.
- (16) Guiochon, G.; Felinger, A.; Katti, A. M.; Shirazi, D. G. *Fundamentals of Preparative and Nonlinear Chromatography*; Elsevier: Amsterdam, 2006.
- (17) Quartapelle Procopio, E.; Linares, F.; Montoro, C.; Colombo, V.; Maspero, A.; Barea, E.; Navarro, J. A. R. *Angew. Chem., Int. Ed.* **2010**, *49*, 7308.
- (18) Diaz, E.; Ordoñez, S.; Vega, A. J. *Colloid Interface Sci.* **2007**, *305*, 7.
- (19) *Gulf War and Health, Volume 1: Depleted Uranium, Sarin, Pyridostigmine Bromide, Vaccines*; Fulco, C. E., Liverman, C. T., Sox, H. C., Eds.; National Academy Press: Washington, DC, 2000.
- (20) Gomez de Salazar, C.; Sepúlveda-Escribano, A.; Rodríguez-Reinoso, F. *Adsorption* **2005**, *11*, 663.